Electronic localization of quantum-well states in Ag/Au(111) metallic heterostructures

F. Forster,[1,*] E. Gergert,[1] A. Nuber,[1] H. Bentmann,[1] Li Huang,[2,3] X. G. Gong,[2] Z. Zhang,[4,5] and F. Reinert[1,6,†]

[1]*Universität Würzburg, Experimentelle Physik VII and Röntgen Research Center for Complex Materials RCCM, Am Hubland, D-97074 Würzburg, Germany*

[2]*Surface Physics Laboratory and Department of Physics, Fudan University, Shanghai 200433, People's Republic of China*

[3]*Ames Laboratory, U.S. Department of Energy, Ames, Iowa 50011, USA*

[4]*Department of Physics and Astronomy, University of Tennessee, Knoxville, Tennessee 37996, USA*

[5]*ICQD/HFNL, University of Science and Technology of China, Hefei, Anhui, 230026, People's Republic of China*

[6]*Karlsruher Institut für Technologie KIT, Gemeinschaftslabor für Nanoanalytik, D-76021 Karlsruhe, Germany*

(Received 22 March 2011; published 3 August 2011)

We report on a detailed analysis of the evolution and spatial localization of quantum-well states (QWSs) in Ag layers on a Au(111) substrate by means of high-resolution photoelectron spectroscopy combined with model calculations based on a simple particle-in-a-box picture, the phase accumulation model, and density functional theory-based slab-layer calculations. Due to the finite electron escape depth we could link the photoemission intensity of the QWS to the simulated charge-density distribution and therewith confirm the calculated localization of these states. The first QWS starts to be localized within the Ag film at layer thicknesses >7 ML.

DOI: 10.1103/PhysRevB.84.075412 PACS number(s): 73.20.At, 68.43.−h, 79.60.Dp

I. INTRODUCTION

The existence or absence of electronic states next to the Fermi level of solids is of fundamental importance for many characteristic properties of the material. In addition, if the surface of the solid is taken into account, the spatial localization of such electronic structures plays a crucial role, e.g., for physical and chemical processes at crystal surfaces such as surface relaxations,[1,2] the growth of adsorbates,[3,4] or even chemical reactivity.[5–7] Therefore it is necessary not only to study the density of states (DOS) but also the spatial charge distribution at or next to the surface. Particularly, electrons in the so-called Shockley states on the noble-metal surfaces of Cu, Ag, and Au(111) behave as free delocalized electrons along the surface plane. However, they are confined in the direction perpendicular to the surface and therefore are a model system for investigations on localized electronic structures.[4,8,9]

Additionally, in a thin film the electrons are spatially confined between the interface to the substrate and the vacuum. Thin epitaxial noble-metal layers on a metallic substrate have become a model system for the investigation of confined electrons in so-called quantum-well states (QWSs) of layered systems such as, e.g., Ag on Cu,[10–12] Au,[13–15] Ni,[16,17] W,[18] and Fe surfaces,[19–22] Au films on W,[18,23,24] and Ru (Ref. 25) as well as Cu on W (Ref. 18) and on a Co substrate.[22,26] An important condition for the confinement of the electrons in the film is the existence of the corresponding bulk states of the adsorbate material at a simultaneous absence of bulk states with the same symmetry in the substrate, meaning a (relative) symmetry band gap. If bulk states of the adsorbate and the substrate with the same symmetry overlap, the adsorbate electrons lose more or less their confinement and become so-called quantum-well resonances (QWRs). The discrimination between QWSs and QWRs is somehow arbitrary and the transition from one to the other is fuzzy since the definition of overlapping states allows a wide range of interpretation.

In this paper we present a systematic photoemission spectroscopy (PES) study on the energetic evolution of the electrons in *sp*-like QWSs and on their confinement in thin Ag/Au(111). Additionally, we performed *ab initio* slab-layer calculations in the framework of density functional theory (DFT) as well as model calculations based on the phase accumulation model (PAM) introduced by Pentry and Echenique[27] for illuminating the experimental findings on the energetic and spatial localization of the Ag QWS.

According to the Bohr-Sommerfeld quantization condition for the existence the of confined *sp*-like electrons in the Ag film, the total accumulated phase of an electron in that film has to be a multiple of 2π. This phase is binding energy dependent and given by the sum of the phase shift at the substrate-film interface $\Phi_C(E_B)$, the phase shift at the surface $\Phi_B(E_B)$, and the accumulated phase during the propagation of the electron through the adsorbed film. This results in the central equation within the PAM,

$$\Phi_C(E_B) + \Phi_B(E_B) + 2dk_\perp(E_B) = 2\pi n, \qquad (1)$$

where $k_\perp(E_B)$ and $d = Na_{\mathrm{ML}}$ reflect the perpendicular dispersion (along the Γ-L direction in the bulk Brillouin zone) of the *sp*-like Ag(111) states and the thickness of a N ML Ag film with a layer distance a_{ML}, respectively.

Therefore, a systematic photoemission study of the energetic evolution of the QWS with increasing Ag film thickness allows to calculate the energy dispersion $E_B(k_\perp)$ of the *sp*-valence states of Ag. This approach is the only possibility for photoelectron spectroscopy to determine electron dispersion perpendicular to the surface unless a tunable photon source is available. Additionally, one can get the energy dependence of the sum of the phase shifts on the substrate-film and film-vacuum interfaces being the starting point for the modeling of the charge-density distribution and for the analysis of QWS localization and the comparison with a particle-in-a box as well as with DFT results. According to our knowledge a direct experimental access to the QWS localization is not possible. In this paper, however, we demonstrate that the photoemission intensity of the QWS of Ag/Au(111) gives an indirect indication of the evolution of the charge-density

distribution in the Ag QWS as a function of film thickness N being consistent with the calculated electron density.

II. EXPERIMENTAL DETAILS

The photoemission experiments have been performed by angle-resolved photoelectron spectroscopy (ARPES) with high-energy resolution ($\Delta E \approx 5$ meV) using a hemispherical analyzer (Gammadata, R4000) and a monochromatic He discharge lamp[28] with a photon energy of 21.2 eV. The base pressure of 1×10^{-10} mbar increases slightly to 8×10^{-10} mbar due to the He flow during the operation of the photon source. This and the moderate sample temperature of 60 K during the measurements reduce the aging of the surface by adsorption of residual gases while the temperature-induced broadening of surface and quantum-well states by electron-phonon interaction remains small.[29–31]

The Au(111) sample was prepared by standard sputtering and annealing cycles described elsewhere[29] until the binding energy and linewidth of the spin-orbit split Shockley state had reached its maximum and minimum values, respectively. Ag has been evaporated by a resistively heated Knudsen cell at 1200 °C on the Au surface. During the evaporation the sample temperature was kept at ~200 K, followed by postannealing at room temperature. This procedure allows a reordering of the very mobile Ag adatoms and a smooth layer formation while an alloying of Ag with the Au surface is avoided.

The evaporation rate of ~0.8 ML per minute was controlled by a standard quartz microbalance. The cleanliness and thickness as well as the quality of the Ag film has been verified by x-ray photoemission and low-energy electron diffraction, respectively. A more precise determination of the film thickness can be done directly from the spectroscopy of surface and quantum-well states as discussed below.

III. RESULTS

A. Evolution of the Shockley state

Figure 1 shows ARPES data of the Au(111) Shockley state before (a) and after a Ag coverage of one (b) and two (c) closed monolayers. The quasi-free-electron behavior becomes obvious in the nearly perfect parabolic band dispersion in neglecting slight deviations close to the Fermi energy E_F due to many-body effects.[32] In all grayscaled plots one clearly observes the L gap of Au bulk states (bright area), indicating a defect-free noble-metal interface. After Ag deposition the typical herringbone ($22 \times \sqrt{3}$) reconstruction of the clean Au(111) (Refs. 33 and 34) visible by backfolded surface-state bands (see arrows) disappears.

With increasing Ag coverage N the Au surface state shifts toward lower binding energies $E_{B,\max}$, whereas its effective band mass m^* increases. The characteristic $k_\parallel$ splitting of the bands is due to the spin-orbit coupling in Au and decreases but is still resolvable for 2 monolayer (ML) Ag/Au(111). The evolution of the Shockley state as a function of Ag film thickness is intensely discussed in the literature in terms of a potential change at the surface and an increasing Ag character due to its surface localization,[35,36] confirmed by DFT-based slab-layer calculations.[37]

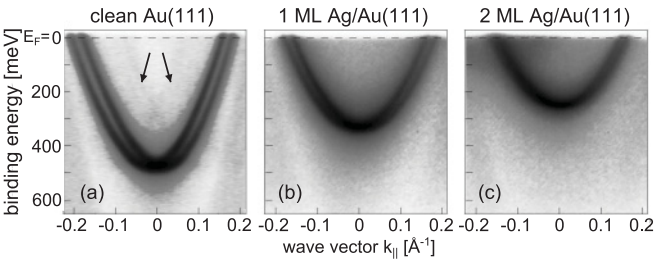

FIG. 1. PES data on the surface state of clean (a) and covered Au(111) with one (b) and two Ag ML (c). The maximum binding energy $E_{B,\max}$ and the Rashba-like spin-orbit splitting decrease with Ag coverage while the band mass m^* increases. The band gap of the Au bulk states (bright area) remains visible and indicates a high signal-to-noise ratio, suggesting a well-ordered and nearly defect-free Ag growth. The weak backfolded Au bands (arrows) caused by the herringbone reconstruction disappear.

The layer-by-layer growth of Ag on Au(111) can be observed via surface-state measurements on various coverages up to $N \approx 7$ ML. Figure 2(a) shows EDCs of the surface state in normal emission (at $\overline{\Gamma}$, $k_\parallel = 0$) together with Lorentzian fits to the experimental data. For noninteger Ag coverages $N = n + x$ ($n \in \mathbb{N}, 0 \leqslant x < 1$), one can clearly distinguish between the two energy-separated Shockley states being connected with n ML and $(n + 1)$ ML Ag/Au(111), respectively. Thus, a quite precise Ag film thickness determination is possible by considering the surface-state intensity ratio.[15] For larger coverages $N > 7$ ML the further surface-state shift gets significantly smaller, meaning a less accurate separation of the nth and $(n + 1)$th Ag monolayer. Therefore an exact determination of the Ag-film thickness N by consideration of the respective surface states is not possible anymore.

B. Evolution of quantum-well states

Figure 2(b) shows a blowup of the energy range of the L-gap edge. Bulk sp states become obvious as an enhanced

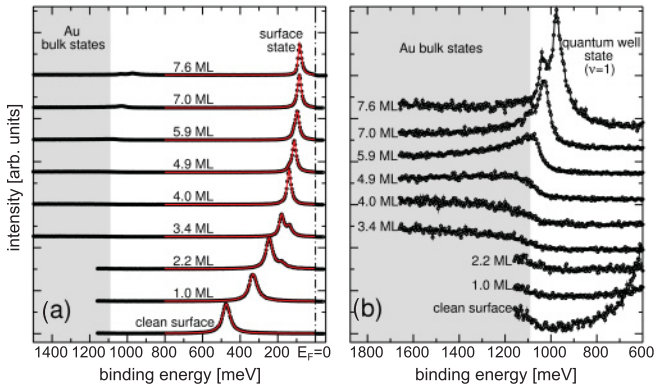

FIG. 2. (Color online) Energy distribution curves at normal emission ($k_\parallel = 0$) of clean and N ML thick Ag films on Au(111). (a) The surface-state shifts in discrete steps with increasing Ag coverage N to lower binding energies is an indication of a layer-by-layer growth. (b) A closer look at the binding energy region at the Au gap edge ($E_{B,\text{gap}} = 1090$ meV) shows the evolution of the first QWS ($v = 1$). At Ag coverages $N \geqslant 7$ it is situated within the Au band gap and shifts in discrete steps to lower bindings energies as well.

photoemission intensity at binding energies is >1090 meV. The increased intensity in the spectrum of the clean substrate arises from the tail of the Au(111) Shockley state. At Ag coverages $N \geqslant 5$ ML, a unique feature becomes apparent and shifts above the Au gap edge at $N = 7$ ML. This unique state can be identified as the first ($\nu = 1$) *sp*-like QWS of the Ag film. The surface state before this state also shifts in discrete steps to lower binding energies, indicating a layer-by-layer growth even at Ag coverages of $N > 7$ ML.[15] While a similar behavior is known for Ag/Fe(100) up to ∼100 ML[21] this discrete QWS shift for Ag/Au(111) is found up to 25 ML.

Although the Ag QWS has a nearly perfect Lorentzian line shape inside the Au band gap, there are distinct deviations close to the gap edge at $N = 5,6,7$ ML Ag coverages. These results give reason to the assumption of a strong influence of many-body effects which was already discussed for QWSs in Ag films on Ge(111).[38] Furthermore, the energetic overlap of the Ag QWS with the Au bulk states gives reason to speculate about a reduced photohole lifetime due to a strongly increased interaction between the Ag QWS and Au *sp* bands.

With increasing Ag coverage the ($\nu = 1$) QWS shifts further into the *L* gap of Au(111). At a film thickness of $N =$ 17 ML, a second QWS ($\nu = 2$) arises within the bulk band gap and further states become obvious at higher Ag coverages. In Fig. 3 a series of data on Ag film thicknesses of $N = 13.5$, 19.5, 27, and 36 ML on Au(111) is presented, showing the photoemission intensity in grayscaled plots as a function of binding energy E_B and emission angle Θ. For a better illustration the grayscale has been adjusted to display both the surface-state dispersion and the much less intense QWS and resonances. The band gap of the Au(111) substrate remains visible as well (bright area), even at large Ag coverages. Similar to the surface states, the QWSs show a parabolic dispersion with a maximum binding energy at normal emission ($\Theta = 0$). It is worth noting that their band curvature of the parabola is considerable smaller than the curvature of the Au band gap edge. Consequently the QWSs cross the bulk gap edge and become resonances as clearly seen, e.g., in the 13.5- and 19.5-ML Ag/Au(111) system for the ($\nu = 1$) state at $\Theta \approx \pm 5^\circ$ and for the ($\nu = 2$) state at $\Theta \approx \pm 4^\circ$, respectively.

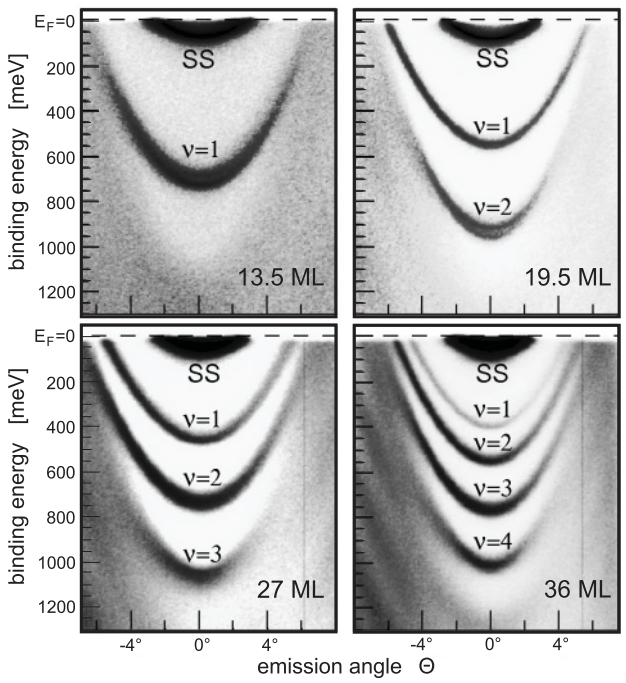

FIG. 3. Grayscale plot of photoelectron intensity of *N* ML Ag/Au(111) as a function of binding energy E_B and emission angle Θ at various film thicknesses. The intensity has been scaled to visualize both the parabolic dispersion of the surface state and the less intense QWSs. Beside the Au substrate band gap (bright area), quantum-well resonances are visible beyond the gap, particularly at larger Ag coverages. Note that even at 19.5-ML Ag the layer-by-layer growth is obvious.

C. Phase accumulation model

In the following discussion we focus on the photoemission results obtained in normal emission to study the energetic evolution of the QWS. In Fig. 4 the maximum binding energy $E_{B,\max}$ of the surface state and the QWS ν is presented as function of Ag overlayer thickness *N*. As discussed in the Introduction, the PAM applied to the energetic evolution of these Ag QWSs can be used for the determination of the $k_\perp$ dispersion [along the *L* direction in the three-dimensional (3D) Brillouin zone] of the Ag(111) *sp*-bulk state and the total phase shift Φ_{tot}. For different QWS $\nu_{i,j}$ using Eq. (1) and $\nu = N - n$, one obtains

$$\Phi_{\text{tot}}(E_B) = \Phi_C(E_B) + \Phi_B(E_B) = 2\pi \frac{N_i \nu_j - N_j \nu_i}{N_j - N_i} \quad (2)$$

and

$$k_\perp(E_B) = \frac{\pi}{a_{\text{ML}}} \left(\frac{\nu_i - \nu_j}{N_j - N_i} + 1 \right). \quad (3)$$

Figure 4(a) displays the results on the total phase shift Φ_{tot} as function of binding energy E_B. The solid line represents a square-root fit to the data according to Refs. 39 and 40. The PAM analysis is completed with the results on the dispersion

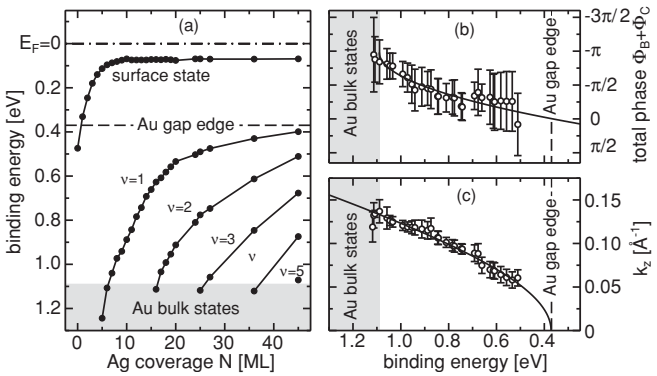

FIG. 4. (a) The maximum binding energy $E_{B,\max}$ of the surface state and the first five QWSs ν as a function of Ag film thickness *N*. The energy range of the Au bulk states is gray shaded. With increasing coverage the QWSs close ranks and asymptotically approach the edge of the Ag bulk band gap (dashed line). According to the phase accumulation model with Eqs. (2) and (3) one can calculate the total phase shift $\Phi_{\text{tot}}(E_B)$ (b) and the $k_\perp$ dispersion (c) of the *sp*-bulk state of Ag(111) in the Γ-*L* direction of the bulk Brillouin zone, respectively.

of the Ag(111) sp band. The origin ($k_z = 0$) has been chosen to be identical with the L point in the 3D Brillouin zone boundary at 1.33 Å^{-1}. The straight line represents a fit to the determined data points considering a nearly free-electron dispersion with a band mass $m^* = (0.66 \pm 0.05)m_e$ being in agreement with earlier results on QWSs in Ag on Cu(111) and Au(111).[10,41] Additionally, the minimum binding energy of the bulk state [$E_B = (370 \pm 10)$ meV] confirms the value of the lower band-gap edge of clean Ag(111) at $\overline{\Gamma}$ in the projected surface Brillouin zone.

IV. SPATIAL LOCALIZATION OF THE Ag/Au(111) QUANTUM-WELL STATES

In addition to the electronic band structure of the Ag layers, one can deduce the spatial localization of the QWSs. In the following we discuss the systematic investigation on deviations of the QWS from a simple particle-in-a-box scenario by taking the phase shift into account, which was determined before. Furthermore, we present studies on its spatial evolution by DFT-based slab-layer calculations and compare the results to observations of the integrated PE QWS intensity.

A. Infinite potential well

In the simplest picture an electron of a QWS can be treated as a particle in a box of infinitely high potential barriers. In Fig. 5 the normalized probability density $\rho_\nu(z) = |\Psi(z)|^2$ of the first ($\nu = 1$) QWS (equivalent to the charge density for occupied states) is plotted (upper lines) for different well

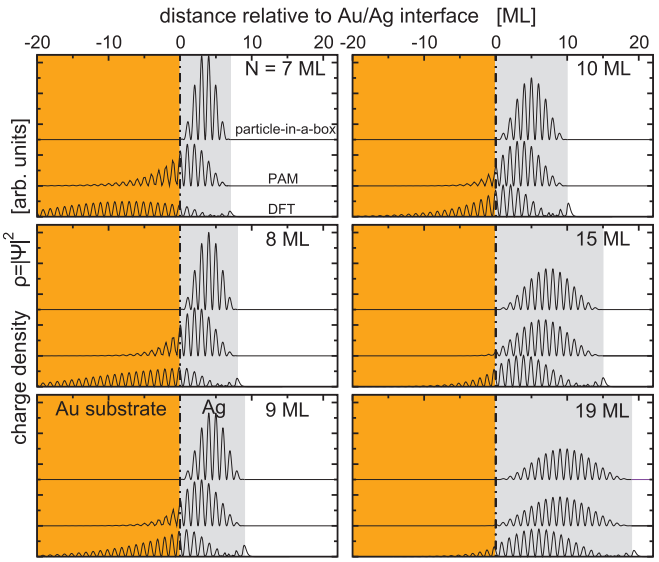

FIG. 5. (Color online) Comparison of the calculated charge density $\rho_{\nu=1}$ of the first QWS by DFT (bottom) with the two discussed model calculations for a particle in a box (top) and its modification due to phase-shift considerations (middle) for various Ag coverages N. Note that the Bloch-like oscillations due to the periodic atom layers are added. For thicker films the results of the extended particle-in-a-box model as well as the DFT calculated charge density become more symmetric and converge to the ($\nu = 1$) state of an infinite potential well.

expansions or Ag film thicknesses. Note that the Bloch-like oscillations due to the periodic Ag layers in the films are added for clarity. An enlargement of the Ag coverage causes an expansion of the potential well and of the state, which becomes more and more uniformly distributed in the Ag film. However, the symmetry with respect to the center of the Ag layer remains unchanged for all coverages N.

Due to the fact that the two potential barriers of the Ag film (toward the Au substrate and vacuum) are neither infinite nor identical, and the phase of the QWSs show a significant binding energy E_B dependence [compare $\Phi_C(E_B) + \Phi_B(E_B)$ in Fig. 4] the very simplified model has to be accurately adjusted.

B. Consideration of phase shift Φ_C and Φ_B

In the considered binding energy region 1090 meV $> E_B >$ 370 meV and for Ag coverages >5 ML, the change of the potential barrier and therefore the change of the induced phase shift at the Ag layer-vacuum interface is negligible and $\Phi_B(E_B) \approx$ const. For simplicity, we adhere to the infinite barrier between the Ag layer and vacuum and fix $\Phi_B(E_B) = -\pi$. However, the barrier on the Au substrate and Ag film becomes finite and determines the phase-shift dependence Φ_C on the binding energy E_B of the QWS.

Hence, the charge density $\rho_\nu(z) = |\Psi_\nu(z)|^2$ of the Ag QWS is a function of binding energy E_B being itself dependent on the Ag film thickness N, as discussed before. It can be calculated by taking into account the determined phase shift $\Phi_C[E_B(N)]$ (see Fig. 4) as well as the matching condition of wave function $\Psi_\nu(z = 0)$ and its derivative $\frac{\partial \Psi_\nu(z)}{\partial z}|_{z=0}$ at the Ag/Au interface. In Fig. 5 the results of the charge-density distribution of the ($\nu = 1$) QWS for different Ag film thicknesses N are presented as solid lines. Note that within these PAM results the formation of bound states is only possible for $N \geqslant 7$ ML. Whereas the state according to the model of the infinite potential well is always completely localized in the Ag film, there are significant differences for the same state obtained by the modified model. Especially for small Ag coverages $N < 15$ ML a non-negligible fraction of the charge density $\rho_{\nu=1}$ is localized inside the Au substrate. Only at larger Ag film thicknesses (e.g., $N = 19$ ML) the ($\nu = 1$) QWS obtained by both models are similar and (almost) completely localized in the Ag layers.

C. Slab-layer calculations

In order to get a deeper insight into the energetic evolution and into the spatial localization of the QWSs, we carried out *ab initio* DFT-based slab-layer calculations within the generalized gradient approximation (GGA) using the VASP code.[42–45] For modeling the Ag-layer systems on a Au(111) surface a periodic slab has been constructed consisting of at least 25-ML Au with N Ag adlayers and a vacuum region of 25 Å separating the slabs. Further details of the calculations including slab relaxation can be found in Ref. 14.

Figure 5 shows the obtained DFT results (bottom panel) on the bulklike electronic state with the smallest binding energy at the $\overline{\Gamma}$ point of the surface Brillouin zone.[14] They are compared with the infinite potential well model (top panel)

and its modification due to the phase accumulation model (middle panel) for a variety of different Ag film thicknesses N. The DFT results are illustrated as the plane-averaged charge-density distribution $\rho(z) = |\Psi(z)|^2$ of the respective energy eigenvalues.[14] The envelope of the charge density is superposed on layer spaced oscillations due to the Bloch-like character. At low coverages the state is delocalized over the whole Au slab and only a small fraction lies within the Ag film. With increasing Ag thickness the state gradually shifts out of the Au bulk and carries more weight inside the Ag layers. At larger Ag layer thicknesses the envelope of the charge density takes the shape of a true ($\nu = 1$) QWS and is comparable with the results discussed before. Below $N \approx 7$ ML the state is situated within or next to the energy range of Au bulk states and therefore not identifiable as a Ag QWS. It is worth noting that this result is consistent with the experimentally determined Ag coverage at which the ($\nu = 1$) QWS develops in the Au bulk band gap. It should also be mentioned, that the distinct feature at the Ag-vacuum interface is not a surface state but the contribution of the QWS to the charge density at the surface.

D. Quantification of QWS localization

As a measure of the QWS localization one can consider the fraction of charge in the Ag film p_{Ag}. This is determined by the normalized charge-density distribution $\rho(z)$ using

$$p_{\mathrm{Ag}}(N) = \int_{z_0=0}^{\infty} \rho_N(z')dz'. \tag{4}$$

The lower integration limit $z_0 = 0$ is fixed to be the interface between the Au substrate and Ag film. Due to the fact that the upper limit is not realizable for a final slab, the integration is aborted since the charge density beyond the surface vanishes.

In Fig. 6 the fraction of charge of the first QWS inside the Ag p_{Ag} is displayed as function of film thickness N. Since for the model of a infinite potential well the complete charge is localized in the Ag layers for all thicknesses (dashed line), the results considering the PAM as well as the DFT calculations show distinct thickness dependences. Only with increasing Ag layers N the fraction of charge within the film converges to the limit $p_{\mathrm{Ag}}(N \to \infty) = 100\%$.

For a better illustration of the QWS localization, Fig. 6(a) shows the Ag coverage dependence of the maximum position $z_{\max}$ and the center of charge z_c being calculated by

$$\int_{z_c}^{\infty} \rho_N(z')dz' = \frac{1}{2}. \tag{5}$$

In the case of an infinite potential well, both the maximum position and the center of charge coincide within the middle of the Ag film, resulting in a gradient of $\frac{dz}{dN} = \frac{1}{2}$. The finding from the quantum-well model considering the energy-dependent phase shift $\Phi_C(E_B)$ shows a significant discrepancy for small Ag films but an asymptotic convergency to the values of the infinite potential for thicker films. Furthermore, the DFT calculated results are included. Here, the center of charge and maximum position show a crossing of the Au/Ag interface $z = 0$ at 8 and 10 ML, respectively. For larger Ag layers the gradient $\frac{dz}{dN}|_{N>10} \approx \frac{1}{2}$ is in agreement with the value for the infinity potential well. The only difference is a constant offset due to the nondisappearing charge fraction in the Au substrate.

Both the maximum position of the charge distribution and the center of charge with $z_{\max} > 0$ and $z_c > 0$, respectively, can be used as unique criteria for the determination of the evolution of QWS from resonant states. According to that, one can determine the formation of the ($\nu = 1$) QWSs within the DFT calculations since the energy criterion fails, as discussed before. We get critical Ag layer thicknesses of $N_{\nu=1} = 8$ and 10 ML for the maximum position and center-of-charge criterion, respectively, being in agreement with the experimental result of 7 ML. Furthermore, analogous calculations on the second ($\nu = 2$) QWSs have been performed and result in a critical Ag layer thickness of $N_{\nu=2} = 19$ ML for its formation, similar to our spectroscopic determined value of 17 ML.

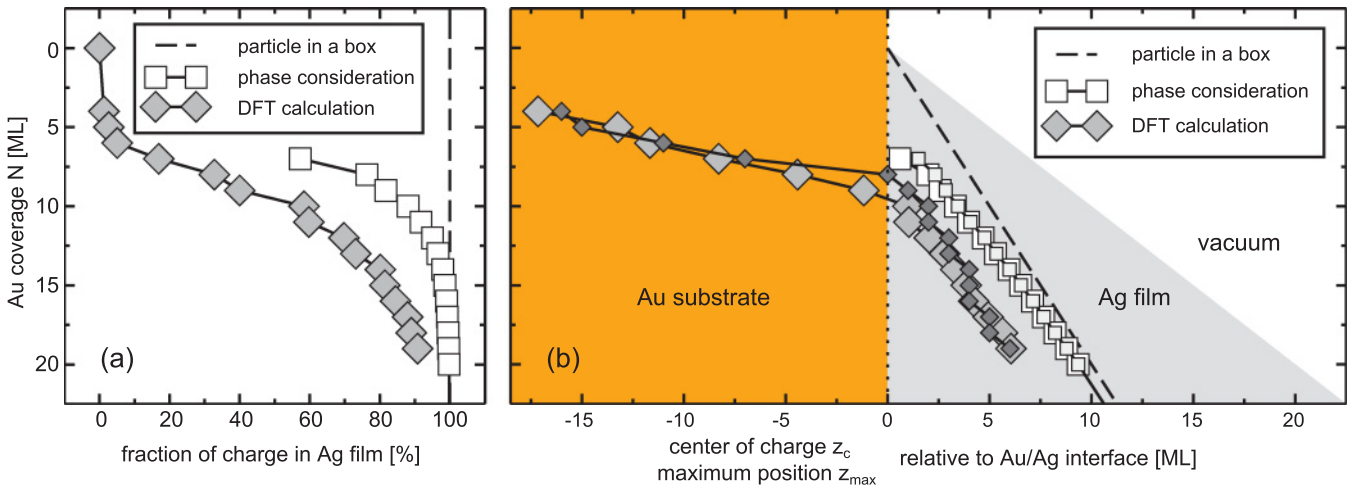

FIG. 6. (Color online) (a) Fraction of charge of the first QWS ($\nu = 1$) inside the Ag film as a function of film thickness N. The results determined by model calculation considering the phase shift (□) and obtained by DFT calculations (◊) approach a value of 100% with increasing Ag coverage. (b) For determination of the spatial QWS evolution, the center of charge (large symbols) and the maximum position (small symbols) are displayed against the Ag film thickness N. For large coverages the curve progressions approach the middle of the film, where the QWS of an infinite potential well is localized.

E. Experimental determination of the localization of quantum-well states

Although an experimental determination of the spatial localization of electronic states within and above a surface is possible, e.g., in terms of scanning tunneling microscopy (STM),[46] we are not aware of a method for directly measuring the state localization inside a film or a hidden interface. However, the PES permits an indirect access due to its surface sensitivity, as demonstrated in the following. The initial point is the escape depth or the inelastic mean free path λ of photoelectrons being in the order of magnitude of only a few Å. It depends on their kinetic energy E_{kin} but is nearly constant for different materials within the universal curve.[47] For the detected energy region of the Ag QWSs, we have $E_{\mathrm{kin}} \approx 16$ eV and used $\lambda = 4$ ML, being in agreement with the experiment value of 10 Å or 4.32 ML for Ag(111).[48] Therefore, the photoemission final state $\Psi_f(z)$ can be approximated to be an exponentially damped function independent of all Ag coverages N on the Au(111) substrate.

In a first-order approximation the photoemission intensity I is determined by the integrated charge density weighted by the exponentially decreased probability of photoelectron escape[47,49] and one gets

$$I_\nu(N) \propto \int_{-\infty}^{\text{surface}} e^{\frac{z'}{\lambda}} \rho_{\nu,N}(z')dz'. \tag{6}$$

Thus, for differently localized states $\Psi_{\nu,N}(z)$ but with the same symmetry (here *sp* like), the PES detects different intensities being suitable to gain information about the QWS localization of the Ag/Au(111) interlayer system.

For this we determined the integrated PES intensity of the QWS resulted from a fit of several Lorentzian peaks on the EDCs at normal emission for different Ag layer thicknesses as shown in Fig. 7(a) for a $N = 45$ ML thick film. We normalized all spectra to the respective surface state which does not show a significant change at Ag coverages $N > 7$ ML, as shown before. The Ag film quality and its surface exhibit different defect densities due to marginally varied preparation conditions. Contrary to the linewidth and the binding energy position the integrated intensity change of the surface state is negligible.[30] Therefore, a direct comparison of the PES intensity of QWS on different Ag film thicknesses is possible.

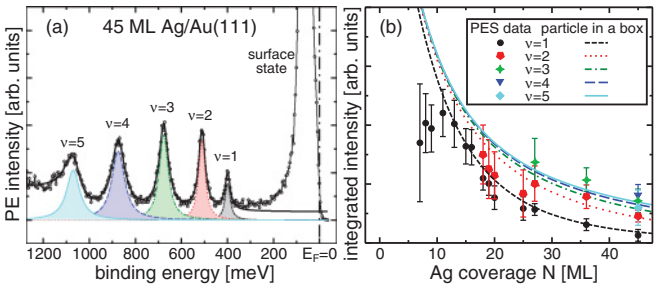

FIG. 7. (Color online) (a) EDC at normal emission ($k_\parallel = 0$) of a 45-ML-thick Ag film on Au(111). The colored lines represent least-square fits of Lorentz peaks on the QWS $\nu = 1, \ldots, 5$. The intense state near the Fermi level is the Ag-like surface state. (b) shows the integrated intensity I_ν of the Lorentz peaks of the QWS (normalized to the surface-state intensity) as a function of Ag film thickness N. The dashed colored lines represent fits of the calculated function $I_\nu(N)$ on the data $n \geqslant 18$ according to Eq. (6) for QWSs of an infinite potential well and assuming an photoelectron escape depth of $\lambda = 4$ Å. At Ag coverage $N < 10$ ML there are significant deviations between experimental data and the model calculations.

Figure 7(b) displays the integrated and normalized intensity of the QWS $\nu = 1, \ldots, 5$ as function of Ag coverage N. It is obvious that the intensity of the states increases with the quantum number ν at a given film thickness. Furthermore, the data for a fixed ν at $N > 10$ ML show a continuously decreasing photoemission intensity with increasing Ag coverage approving the evolution of QWS delocalization within the Ag film. For comparison we added the calculated curve progression according to Eq. (6) for the electrons in an infinite potential well. This simple model reproduces the experimental data for thicker Ag films with a significant deviation for Ag coverages $N < 11$ ML. The reduced photoemission intensity of the ($\nu = 1$) QWS for coverages $N < 11$ ML indicates an enhanced delocalization of the state into the Au substrate being not described within the infinite potential well model.

We performed calculations in the same way for the ($\nu = 1$) QWS intensity according to the asymmetric potential well due to the PAM. In Fig. 8(a) the results are displayed together with the experimental data as well as with the results within the infinity potential well model calculations. One observes deviations between the two models only for lower Ag coverages and finds a better agreement of the experimental values with the extended model even for thinner Ag films. Particularly, the increased QWS delocalization for lower coverages is here more accurately reproduced.

Figure 8(b) shows a comparison between the photoemission intensity concerning the ($\nu = 1$) QWS and the results according to the slab-layer calculations and Eq. (6). The agreement of the experimental values and theory is obvious. In particular, the calculations accurately describe the rediminishment of the intensity for Ag coverages $N < 11$ ML. Thus we conclude that the calculated charge density of the QWS $\rho_{\nu=1,N}(z)$ approaches its real localization within the Ag film. Nevertheless, an absolute confirmation of the spatial evolution of the ($\nu = 1$) QWS or even its direct determination by photoemission

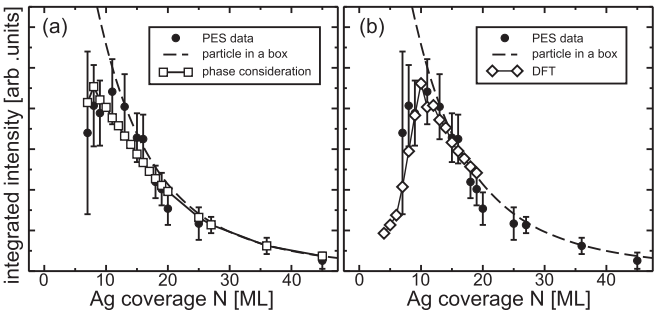

FIG. 8. Integrated photoelectron intensity of the first QWS of Ag/Au(111) against film thickness N (•). (a) and (b) show the comparison of the experimental data to model calculations considering the phase shift (□) and to the results obtained by DFT calculations (◊), respectively. Both calculations show a significantly better agreement with the experimental results than the simple model of a particle-in-a-box added as dashed lines. Particularly, the maximum intensity at $N \approx 10$ is reproduced for the DFT-based model calculations.

intensity investigations are not possible since the investigations cover the weighted integral over the z coordinate [see Eq. (6)] but not directly the charge density $\rho_{\nu,N}(z)$.

V. CONCLUSION

To summarize, we performed a detailed investigation on the evolution and spatial localization of quantum-well states in Ag layers within the L gap of a Au(111) substrate. Therefore we utilized high-resolution photoelectron spectroscopy and its surface sensitivity in combination with calculations of a particle in a box, the phase accumulation model and DFT-based slab-layer calculations. To our knowledge this is, even though indirect, a technique to determine the spatial localization of electronic states within a solid film.

The measured photoemission intensity variation of the QWS originating from different film thicknesses, caused by the finite electron escape depth and spatial localization of the charge density, matches the according simulation based on DFT slab-layer calculations. Herewith we could confirm the calculated charge-density distribution and discriminate quantum-well states and quantum-well resonances by the criterion of center of charge z_c or maximum position of the charge density $z_{\max}$. The film thickness when z_c or $z_{\max}$ starts to be localized within the Ag film matches the $\sim$7 ML when the first QWS appears within the L gap in photoemission data.

ACKNOWLEDGMENT

This work was supported generously by the Deutsche Forschungsgemeinschaft (Grants No. FOR 1162 and No. Re1469/5-1), the BMBF (05KS7WW1Y2), and in part by the US National Science Foundation (Grant No. 0906025).

*Present address: Staatliches Studienseminar für das Lehramt an Gymnasien und Gesamtschulen, Saarland, St. Nazairer Allee 6, D-66740 Saarlouis, Germany.

†Corresponding author: reinert@physik.uni-wuerzburg.de

[1] V. Chis and B. Hellsing, Phys. Rev. Lett. **93**, 226103 (2004).

[2] S.-J. Tang, H.-T. Jeng, C.-S. Hsue, Ismail, P. T. Sprunger, and E. W. Plummer, Phys. Rev. B **77**, 045405 (2008).

[3] F. Silly, M. Pivetta, M. Ternes, F. Patthey, J. P. Pelz, and W.-D. Schneider, Phys. Rev. Lett. **92**, 016101 (2004).

[4] F. Forster, A. Bendounan, J. Ziroff, and F. Reinert, Phys. Rev. B **78**, 161408 (2008).

[5] E. Bertel, P. Roos, and J. Lehmann, Phys. Rev. B **52**, R14384 (1995).

[6] M. Kulawik, H.-P. Rust, M. Heyde, N. Nilius, B. A. Mantooth, P. S. Weiss, and H.-J. Freund, Surf. Sci. **590**, L253 (2005).

[7] L. Aballe, A. Barinov, N. Stoji, N. Binggeli, T. O. M. A. Locatelli, and M. Kiskinova, Appl. Phys. **22**, 015001 (2010).

[8] F. Reinert, G. Nicolay, S. Schmidt, D. Ehm, and S. Hüfner, Phys. Rev. B **63**, 115415 (2001).

[9] F. Forster, A. Bendounan, J. Ziroff, and F. Reinert, Surf. Sci. **600**, 3870 (2006).

[10] M. A. Mueller, T. Miller, and T.-C. Chiang, Phys. Rev. B **41**, 5214 (1990).

[11] S. Mathias, M. Wessendorf, S. Passlack, M. Aeschlimann, and M. Bauer, Appl. Phys. A **82**, 439 (2006).

[12] S. Mathias, M. Wiesenmayer, M. Aeschlimann, and M. Bauer, Phys. Rev. Lett. **97**, 236809 (2006).

[13] T. Miller, A. Samsavar, G. E. Franklin, and T.-C. Chiang, Phys. Rev. Lett. **61**, 1404 (1988).

[14] L. Huang, X. G. Gong, E. Gergert, F. Forster, A. Bendounan, F. Reinert, and Z. Zhang, Europhys. Lett. **78**, 57003 (2007).

[15] D.-A. Luh, C.-M. Cheng, K.-D. Tsuei, and J.-M. Tang, Phys. Rev. B **78**, 233406 (2008).

[16] A. Varykhalov, A. M. Shikin, W. Gudat, P. Moras, C. Grazioli, C. Carbone, and O. Rader, Phys. Rev. Lett. **95**, 247601 (2005).

[17] B. V. Senkovskiy, A. Y. Varykhalov, A. M. Shikin, V. K. Adamchuk, and O. Rader, Phys. Solid State **48**, 1974 (2006).

[18] D. V. Vyalykh, A. Shikin, G. V. Prudnikova, A. Y. Grigor'ev, A. G. Starodubov, and V. K. Adamchuk, Phys. Solid State **44**, 164 (2002).

[19] T. Miller, J. J. Paggel, D.-A. Luha, and T.-C. Chiang, J. Electron Spectrosc. Relat. Phenom. **114–116**, 513 (2001).

[20] J. J. Paggel, T. Miller, and T.-C. Chiang, Phys. Rev. Lett. **81**, 5632 (1998).

[21] J. J. Paggel, T. Miller, and T.-C. Chiang, Science **283**, 1709 (1999).

[22] J. E. Ortega and F. J. Himpsel, Phys. Rev. Lett. **69**, 844 (1992).

[23] A. M. Shikin, O. Rader, G.-V. Prudnikova, V. K. Adamchuk, and W. Gudat, Phys. Rev. B **65**, 075403 (2002).

[24] H. Knoppe and E. Bauer, Phys. Rev. B **48**, 5621 (1993).

[25] J. Choi, J. Wu, F. El Gabaly, A. K. Schmid, C. Hwang, and Z. Q. Qiu, New J. Phys. **11**, 043016 (2009).

[26] Y. Z. Wu, A. K. Schmid, M. S. Altman, X. F. Jin, and Z. Q. Qiu, Phys. Rev. Lett. **94**, 027201 (2005).

[27] P. M. Echenique and J. B. Pendry, J. Phys. Condens. Matter **11**, 2065 (1978).

[28] F. Reinert and S. Hüfner, New J. Phys. **7**, 97 (2005).

[29] G. Nicolay, F. Reinert, S. Schmidt, D. Ehm, P. Steiner, and S. Hüfner, Phys. Rev. B **62**, 1631 (2000).

[30] G. Nicolay, F. Reinert, F. Forster, D. Ehm, S. Schmidt, B. Eltner, and S. Hüfner, Surf. Sci. **543**, 47 (2003).

[31] F. Reinert, G. Nicolay, S. Schmidt, D. Ehm, and S. Hüfner, Phys. Rev. B **63**, 115415 (2001).

[32] A. Eiguren, S. de Gironcoli, E. V. Chulkov, P. M. Echenique, and E. Tosatti, Phys. Rev. Lett. **91**, 166803 (2003).

[33] W. Chen, V. Madhavan, T. Jamneala, and M. F. Crommie, Phys. Rev. Lett. **80**, 1469 (1998).

[34] F. Reinert and G. Nicolay, Appl. Phys. A **78**, 817 (2004).

[35] A. Bendounan, H. Cercellier, Y. Fagot-Revurat, B. Kierren, V. Y. Yurov, and D. Malterre, Phys. Rev. B **67**, 165412 (2003).

[36] H. Cercellier, Y. Fagot-Revurat, B. Kierren, and D. M. F. Reinert, Surf. Sci. **566**, 520 (2004).

[37] D. Popović, F. Reinert, S. Hüfner, V. G. Grigoryan, M. Springborg, H. Cercellier, Y. Fagot-Revurat, B. Kierren, and D. Malterre, Phys. Rev. B **72**, 045419 (2005).

[38] S.-J. Tang, L. Basile, T. Miller, and T.-C. Chiang, Phys. Rev. Lett. **93**, 216804 (2004).

[39] M. A. Mueller, E. S. Hirschorn, T. Miller, and T.-C. Chiang, Phys. Rev. B **43**, 11825 (1991).

[40]M. A. Mueller, A. Samsavar, T. Miller, and T.-C. Chiang, Phys. Rev. B **40**, 5845 (1989).
[41]T.-C. Chiang, T. Miller, and W. E. McMahon, Phys. Rev. B **50**, 11102 (1994).
[42]G. Kresse and J. Furthmüller, Comput. Mater. Sci. **6**, 15 (1996).
[43]D. Vanderbilt, Phys. Rev. B **41**, 7892 (1990).
[44]G. Kresse and J. Hafner, J. Phys. Condens. Matter **6**, 8245 (1994).
[45]J. P. Perdew and Y. Wang, Phys. Rev. B **45**, 13244 (1992).
[46]M. F. Crommie, C. P. Lutz, and D. M. Eigler, Nature (London) **363**, 524 (1993).
[47]S. Hüfner, *Photoelectron Spectroscopy*, Springer Series in Solid-State Sciences, Vol. 82 (Springer, Berlin, 1996).
[48]E. D. Hansen, T. Miller, and T.-C. Chiang, Phys. Rev. B **55**, 1871 (1997).
[49]M. Jalochowski, H. Knoppe, G. Lilienkamp, and E. Bauer, Phys. Rev. B **46**, 4693 (1992).